Neuropharmacology 260 (2024) 110130

Contents lists available at ScienceDirect

Neuropharmacology

journal homepage: www.elsevier.com/locate/neuropharm

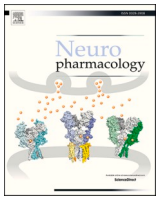

Effects of four-week intranasal oxytocin administration on large-scale brain networks in older adults

Peiwei Liu [a,*], Tian Lin [a], Håkan Fischer [b,c,d], David Feifel [e], Natalie C. Ebner [a,f,g,**]

[a] Department of Psychology, University of Florida, Gainesville, FL, 32611, USA
[b] Department of Psychology, Stockholm University, Stockholm, SE-106 91, Sweden
[c] Stockholm University Brain Imaging Centre (SUBIC), Stockholm University, Stockholm, SE-106 91, Sweden
[d] Aging Research Centre, Karolinska Institute, Stockholm, SE-171 77, Stockholm, Sweden
[e] Department of Psychiatry, University of California, San Diego, CA, 92093, USA
[f] Institute on Aging, University of Florida, Gainesville, FL, 32611, USA
[g] Center for Cognitive Aging and Memory, University of Florida, Gainesville, FL, 32610, USA

A B S T R A C T

Oxytocin (OT) is a crucial modulator of social cognition and behavior. Previous work primarily examined effects of acute intranasal oxytocin administration (IN-OT) in younger males on isolated brain regions. Not well understood are *(i)* chronic IN-OT effects, *(ii)* in older adults, *(iii)* on large-scale brain networks, representative of OT's wider-ranging brain mechanisms. To address these research gaps, 60 generally healthy older adults (mean age = 70.12 years, range = 55–83) were randomly assigned to self-administer either IN-OT or placebo twice daily via nasal spray over four weeks. Chronic IN-OT reduced resting-state functional connectivity (rs-FC) of both the right insula and the left middle cingulate cortex with the salience network but enhanced rs-FC of the left medial prefrontal cortex with the default mode network as well as the left thalamus with the basal ganglia–thalamus network. No significant chronic IN-OT effects were observed for between-network rs-FC. However, chronic IN-OT increased selective rs-FC of the basal ganglia–thalamus network with the salience network and the default mode network, indicative of more specialized, efficient communication between these networks. Directly comparing chronic vs. acute IN-OT, reduced rs-FC of the right insula with the salience network and between the default mode network and the basal ganglia–thalamus network, and greater selective rs-FC of the salience network with the default mode network and the basal ganglia–thalamus network, were more pronounced after chronic than acute IN-OT. Our results delineate the modulatory role of IN-OT on large-scale brain networks among older adults.

1. Introduction

The neuropeptide oxytocin (OT) acts as a neuromodulator on social cognition and social behavior (Meyer-Lindenberg et al., 2011). OT is synthesized in the hypothalamus and processed along axonal projections for posterior pituitary and dendritic release into extracellular space, resulting in both local action and diffusion to distant brain regions, such as the amygdala and insula (Meyer-Lindenberg et al., 2011). One of the most well-documented roles of OT is its involvement in maternal and infant bonding. Additionally, OT is implicated in numerous physiological effects, such as reducing free cortisol levels, lowering blood pressure, inducing analgesia, and promoting wound healing (IsHak et al., 2011).

OT can be administered via diverse routes including intranasal, oral, and intravenous (Phung et al., 2021; Zhuang et al., 2022), but intranasal OT administration (IN-OT) circumvents the blood-brain barrier and is well-suited for the investigation of OT effects on human behavior and brain function (Burmester et al., 2018; Quintana et al., 2018). The majority of current research on IN-OT brain modulation, however, considers activity in isolated regions during a task (Koch et al., 2016; Riem et al., 2011; Zhao et al., 2016). Little is known about IN-OT effects on resting-state functional connectivity (rs-FC), i.e., temporal correlations in spontaneous fluctuations of blood oxygen level-dependent (BOLD) signals at rest, providing valuable insights into the inherent functional organization of the brain (Cabral et al., 2011). Further, the few existing IN-OT functional connectivity studies are mostly limited to coupling between two regions (amygdala and insula, De Cagna et al., 2019, nasal administration of 24 International Units (IUs), amygdala and medial prefrontal cortex, Ebner et al., 2016, nasal administration of 24 IUs; thalamus and amygdala, Koch et al., 2019, nasal administration of 40 IUs; but see Bethlehem et al., 2017, nasal administration of 24 IUs; Brodmann et al., 2017, nasal administration of 24 IUs).

* Corresponding author. Center Dr, Gainesville, FL 32603, USA.
** Corresponding author. 945 Center Dr, Gainesville, FL 32603, USA.
E-mail addresses: peiweiliu@ufl.edu (P. Liu), natalie.ebner@ufl.edu (N.C. Ebner).

https://doi.org/10.1016/j.neuropharm.2024.110130
Received 15 February 2024; Received in revised form 18 July 2024; Accepted 20 August 2024
Available online 23 August 2024
0028-3908/© 2024 Elsevier Ltd. All rights are reserved, including those for text and data mining, AI training, and similar technologies.

Complex brain function, however, is subserved by large-scale brain networks (Bellec et al., 2006), such as the salience network (Menon, 2015), the default mode network (Andrews-Hanna et al., 2014), and the basal ganglia–thalamus network (Haber and Calzavara, 2009; Luo et al., 2012). These networks support social function (Di Simplicio et al., 2009; Grimm et al., 2009; Ince et al., 2023; Kirkpatrick et al., 2014), rendering them particularly likely and effective targets of IN-OT modulation. However, a large-scale network approach (both regarding within as well as between network coupling) to the study of IN-OT brain modulation is nascent (for a recent summary see Liu et al., 2022, nasal administration of 24 IUs) and IN-OT's wider-ranging brain mechanisms of action are still insufficiently understood.

Furthermore, previous IN-OT functional connectivity studies exclusively focused on young and middle-aged adults, despite increasing evidence of age-differential effects of IN-OT on both human brain and behavior (Ebner et al., 2013; Horta et al., 2020; Sannino et al., 2017). One exception is Liu et al. (2022) which comprised young and older participants and found that acute (i.e., single-dose) IN-OT decreased rs-FC of the right insula with the salience network in both age groups as well as of the left amygdala with the salience network in older adults. Acute IN-OT also decreased rs-FC between the angular gyrus and the default mode network in both young and older adults. Note that Liu et al. did not examine effects in the basal ganglia–thalamus network, despite evidence of enhanced rs-FC within this network after acute IN-OT in young adults (Bethlehem et al., 2017; Rocchetti et al., 2014).

Finally, only two studies to date have investigated effects of chronic (i.e., repeated) IN-OT on brain activity (Kou et al., 2022, nasal administration for 3 or 5 days with 24 IUs per day) and rs-FC (Watanabe et al., 2015, nasal administration for 6 weeks with 24 IUs twice a day for a total of 48 IUs per day) in humans, and none in aging. To probe IN-OT's treatment potential, however, determination of chronic IN-OT effects on brain functional connectivity, including among older adults, is warranted (Horta et al., 2020a,b [1]).

To fill these research gaps, the present study examined effects of a four-week chronic IN-OT on both within- and between-network rs-FC of the salience network, the default mode network, and the basal ganglia–thalamus network in a sample of generally healthy older adults. Building on Liu et al. (2022), we also directly compared effects from chronic relative to acute IN-OT on within- and between-network connectivity in older adults; as chronic administration of any bioactive drug may produce either more pronounced or less pronounced (tolerance) effects compared to acute administration (Brusa et al., 2007). Chronic IN-OT's effects may be pronounced over acute effects due to Chronic IN-OT's potential for prolonged exposure to the OT (Peters et al., 2014), increased receptor sensitivity (Zanos et al., 2014), and/or neuroplastic changes linked to a decrease in epigenetic methylation of the OT receptor and an increase in OT receptor expression (Alaerts et al., 2023, nasal administration for 28 days with 12 IUs twice a day for a total of 24 IUs per day).

We expected chronic IN-OT to modulate within- (*Hypothesis 1a*) and between- (*Hypothesis 1b*) network rs-FC for all three networks (i.e., salience network, default mode network, and basal ganglia–thalamus network). We further hypothesized more pronounced effects of chronic than acute IN-OT effects on both within- (*Hypothesis 2a*) and between- (*Hypothesis 2b*) network rs-FC for all three networks. Beyond delineation of the effects of chronic IN-OT on a single specific brain network (within-network) or interaction between two brain networks (between-network), we also explored chronic IN-OT effects on resting-state functional coupling between all three networks using selective rs-FC, a comparatively novel metric referring to specific brain networks displaying stronger connections with distinct networks compared to others, indicative of more specialized, efficient network communication (Simmons et al., 2013; Chan et al., 2014). We did not formulate hypotheses for this outcome measure, however, given the lack of prior literature on this variable in OT and aging.

[1] Note that IN-OT has previously been examined as therapeutic strategy in post-traumatic stress disorder (Giovanna et al., 2020), depression and anxiety disorders (De Cagna et al., 2019), and psychiatric disorders with impaired social functioning such as autism and schizophrenia (Kirsch, 2015; Martins et al., 2022).

2. Methods

2.1. Participants

This paper leveraged data from two datasets. Dataset 1, containing chronic IN-OT data, tested *Hypothesis 1a* and *1b*; Dataset 1 and Dataset 2 combined, with Dataset 1 containing acute IN-OT data, tested *Hypothesis 2a* and *2b* as well as were used for the exploratory analysis regarding selective rs-FC. Both data collection protocols were approved by the university's Institutional Review Board (IRB), registered with clinicaltrials.gov (Dataset 1: NCT02069431; Dataset 2: NCT01823146), and monitored by the IRB, a Data Safety Monitoring Board, and the Food and Drug Administration (FDA; IND 100,860).

Regarding Dataset 1, the larger clinical trial comprised 159 participants, who were recruited through fliers in the community and on the university campus, mail-outs to university participant registries as well as via newspaper ads, the community-recruitment service HealthStreet, and word of mouth. Data was collected between February 2016 and February 2020. Fig. 1 provides an overview of the larger project for Dataset 1 (see Rung et al., 2021 for details). We used data from both pre- and post-intervention visits from Dataset 1.

Analysis of Dataset 1 considered participants with complete resting-state fMRI and T1 data both at pre- and post-intervention. All participants were generally healthy, aged 55 or older, eligible for MRI as well as IN-OT, had a pre-intervention blood pressure <180/100 mm Hg, were fluent in English, able to provide informed consent, not pregnant, and scored 30 or higher on the Telephone Interview for Cognitive Status (TICS; Brandt, Spencer and Folstein, 1988). Primary exclusion criteria included hypersensitivity to IN-OT, a history of hyponatremia or syndrome of inappropriate antidiuretic hormone secretion, use of vasoconstrictors (e.g., desmopressin, pseudoephedrine, or antidiuretic medication), low sodium (<134 mEq/L) coupled with high urine osmolality (>1200 L), psychogenic polydipsia, and excessive cigarette smoking or alcohol consumption, severe claustrophobia, major medical surgery in the past two months, large pieces of metal in the body or any metal in the face or neck, a history of brain surgery or any serious brain damage or disease like aneurysm, stroke, or seizures, and severe forms of current glaucoma, macular degeneration, or cataract (see Rung et al., 2021 for details).

After listwise deletion of missing data and removing images with motion artifacts as well as undifferentiated gray matter/white matter, 60 participants (mean age = 70.12 years, standard deviation = 6.57 years, range = 55–83 years; 68.33% males) were submitted to data analysis. Of these 60 participants, 31 (mean age = 71.45 years, standard deviation = 7.46 years, range = 55–83 years, 67.74% males) were randomly assigned to self-administer chronic IN-OT (24 IUs) twice daily over 28 days, between 7 and 9 am and again between 5 and 7 pm) and 29 participants (mean age = 68.69 years, standard deviation = 5.22 years, range = 58–80 years, 68.97% males) to self-administer Placebo (P) at the same dose and frequency. There were no pre-intervention differences in rs-FC between the chronic IN-OT and P group (ps > 0.05), confirming successful randomization. Table 1 summarizes sample-descriptive information and inference statistics for demographics, mood, health, and cognition by treatment group (IN-OT vs. P) for Dataset 1.

Regarding Dataset 2, the larger clinical trial comprised 105 participants who were recruited via university participant pools, fliers across the community and university campus, and word of mouth. Data collection for Dataset 2 took place between August 2013 and October

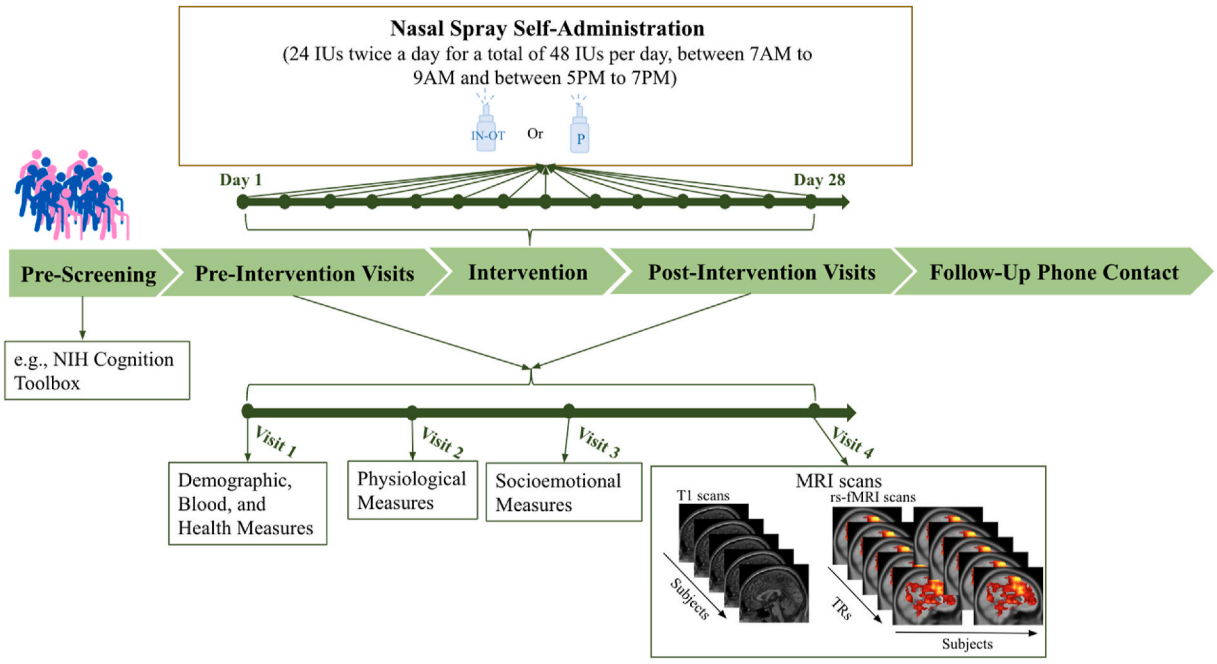

Fig. 1. Overview of Study Flow for Dataset 1 (Chronic IN-OT). Data collection comprised five stages: **Pre-Screening**, to determine participant eligibility; **Pre-Intervention Visits**, involving comprehensive data collection across four visits, including demographic, health, cognitive, physiological, and socioemotional assessments as well as MRI; **Intervention**, with twice-daily administration of 48 international units (IUs) of intranasal oxytocin (IN-OT) or placebo (P) for 28 days; **Post-Intervention Visits**, with data collection identical to pre-intervention visits; and **Follow-Up Phone Contact**, to monitor drug safety and tolerability. **Abbreviations used**: rs-fMRI = resting-state functional Magnetic Resonance Imaging; TRs = Repetition Time. See Rung et al., 2021 for details.

2014. Analysis of Dataset 2 only included older adults with complete resting-state fMRI and T1 data. Eligibility criteria were equivalent to those described for Dataset 1 (see Liu et al., 2022 for details). The final analysis sample included 20 older adults randomly assigned to self-administer 24 IUs IN-OT (mean age = 71.00 years, standard deviation = 6.03 years, range = 63–80 years, 42.86% males). See Liu et al. (2022) for procedure and sample-descriptive information/inference statistics for Dataset 2.

2.2. Procedure

For Dataset 1 (Chronic IN-OT), a phone pre-screening determined general eligibility. After written informed consent, over the following 1–2 weeks participants completed four pre-intervention visits on campus for comprehensive data collection pertaining to physiological, biological, cognitive, and socioemotional measures as well as Electroencephalogram/Event-related potentials (EEG/ERP), eye-tracking, Magnetic Resonance Imaging (MRI), and Magnetic Resonance Spectroscopy (MRS) (see Rung et al., 2021 for details). Here we used the resting-state fMRI data and T1 images. During the resting-state scan, participants were instructed to keep their eyes open and fixate on a centrally presented cross.

During the 28-day intervention phase, participants self-administered 24 IUs twice daily for a total of 48 IUs of IN-OT or P, following standard procedures (Guastella et al., 2013). The study adopted a randomized, double-blinded, between-within subjects experimental design (2 treatment group: chronic IN-OT vs. P as between-subject variable, 2 timepoint: pre-intervention vs. post-intervention as within-subject variable). IN-OT and P were compounded and dispensed by the university Investigational Drug Service under IND 100,860 (see Rung et al., 2021 for safety and tolerability data).

In their last week of nasal spray administration, participants returned to campus for four post-intervention visits which were identical to the pre-intervention visits. Participants were instructed to refrain from administration of the spray the morning of the post-intervention visits, to allow for dissociation of acute from chronic effects, but to continue their self-administration scheme in the evening of testing days. Participants received $350 for study completion, including the imaging components.

For Dataset 2 (Acute IN-OT), a phone pre-screening determined general eligibility, followed by an in-person screen visit on campus to obtain written informed consent and assess demographic, cognitive, and health measures. Two to ten days later, eligible participants returned for a second campus visit during which they self-administered a single-dose (24 IUs) of either IN-OT or P following a randomized, double-blinded, between-subjects experimental design. Participants were then settled into the MRI scanner to obtain T1-weighted anatomical, task-evoked functional, and resting-state functional images (see Ebner et al., 2016; Frazier et al., 2021; Horta et al., 2019; Liu et al., 2022 for details). Here we used resting-state fMRI data and TI images from the older adults in the acute IN-OT group. During the resting-state scan, participants were asked to relax and look at a white fixation cross on a black screen.

2.3. MRI acquisition

In Dataset 1, brain images were acquired on a 3 T Philips Achieva MR Scanner (Philips Medical Systems, Best, The Netherlands). A 32-channel head coil was used with foam padding to reduce head motion. Two-hundred and forty functional images were acquired during an 8-min resting-state scan using a gradient-echo-planar imaging (EPI) sequence with a total of 38 interleaved slices (TR = 2 s, TE = 30 ms, FOV = 252 mm × 252 mm x 133 mm, flip angle = 90°, transverse slice orientation, in plane resolution = 3.5 × 3.5 mm, slice thickness = 3.5 mm without skip). Additionally, high-resolution T1-weighted anatomical images were acquired using a magnetization-prepared rapid gradient echo (MP-RAGE) sequence (sagittal slice orientation, FOV = 240 mm × 240 mm x 170 mm, in plane resolution = 1 mm × 1 mm, slice thickness = 1 mm without skip).

MRI acquisition and task parameters in Dataset 2 (Acute IN-OT) were comparable to those in Dataset 1, except for the in-plane resolution of

Table 1
Sample-descriptive information and inference statistics for Dataset 1 (chronic IN-OT) at pre-intervention.

Characteristics	IN-OT (n = 31)	P (n = 29)	Inference Statistics
Demographics			
Age (yrs, mean (sd))	71.45 (7.46)	68.69 (5.22)	t = −1.67, p = 0.1
Sex (female%)	32.3%	31%	$\chi^2 = 0$, $p = 1$
Race (%)			$p = 0.32$*
American Indian/Alaska Native	3.2%	6.9%	
Asian	0%	0%	
Black/African American	3.2%	13.8%	
White	93.5%	79.3%	
Ethnicity (%)			$p = 0.24$*
Hispanic or Latinx	9.7%	0%	
Education (yrs, mean (sd))	16.32 (2.94)	15.89 (3.40)	t = 0.51, p = 0.61
Mood (mean (sd))			
Positive Affect	47.13 (8.19)	46.52 (9.49)	t = 0.27, p = 0.79
Negative Affect	15.84 (4.24)	16 (4.21)	t = 0.15, p = 0.88
Health (mean (sd))			
Physical	8.29 (1.19)	8.52 (1.15)	t = 0.75, p = 0.46
Mental	8.81 (1.19)	8.72 (0.10)	t = 0.29, p = 0.77
Cognition (mean (sd))			
Crystallized	116.92 (8.65)	118.82 (9.55)	t = 0.69, p = 0.50
Fluid	89.84 (8.41)	91.26 (11.66)	t = 0.54, p = 0.59

Note: **Mood** was assessed using the Positive Affect Negative Affect Schedule (PANAS 20-item short version plus 6 additional adjectives; Röcke et al., 2009; Watson et al., 1988). Participants rated their feelings in general on a scale from 1 = very slightly or not at all to 5 = extremely. Higher mean scores indicated greater levels of Positive Affect and Negative Affect, respectively. **Health** was assessed by asking participants to rate their general physical health (Physical) and their mental health/mood (Mental) on a scale from 1 = poor to 10 = excellent. **Cognition** was assessed using the NIH Cognition Toolbox (Akshoomoff, 2013). Crystallized Cognition and Fluid Cognition were computed utilizing uncorrected composite scores with a normative mean of 100 and a standard deviation of 15, with higher mean scores indicating greater levels of Crystallized Cognition and Fluid Cognition respectively. **Abbreviations used**: yrs = years; sd = standard deviation; % = percentage; $\chi 2$ = chi-square; * indicates use of Fisher's exact test instead of chi-square ($\chi 2$) test to address the issue of inaccurate chi-square approximation caused by small sample sizes or zero counts in the contingency table cell (Campbell, 2007).

the resting-state fMRI scan (3.15 × 3.15 mm) and the FOV in the T1-weighted anatomical images (240 mm × 240 mm x 240 mm; see Liu et al., 2022, for details).

2.4. MRI data preprocessing

The approach described in Liu et al. (2022) was used for MRI data preprocessing for both datasets respectively. In particular, as graphically summarized in Fig. 2A, we used the CONN functional connectivity toolbox (v.18.b; Whitfield-Gabrieli and Nieto-Castanon, 2012) in conjunction with SPM12 software (https://www.fil.ion.ucl.ac.uk/spm/software/spm12/) on MATLAB R2018a (MathWorks Inc., Natick, MA, USA) to preprocess the resting-state MRI images from pre- and post-intervention, following the default preprocessing pipeline for volume-based analysis. Resting-state images were realigned, outlier-removed, unwrapped, slice-timing corrected (interleaved bottom-up), co-registered with T1 images, spatially normalized into MRI space, and smoothed to an 8-mm full width at half maximum (FWHM) Gaussian kernel.

2.5. Independent component analysis (ICA)

The same ICA approach as described in Liu et al. (2022) was applied to Dataset 1 to obtain the targeted brain networks using Group ICA in the fMRI Toolbox (GIFT; http://icatb.sourcefttkorge.net/, version v4.0 b; Calhoun et al., 2009). ICA was performed across pre- and post-intervention data. The protocol comprised *(i)* a component identification and *(ii)* a component selection phase.

As graphically summarized in Fig. 2B, in the component identification phase, ICA was performed in four steps: (1) After data concatenation in time, the data was reduced in dimension using Principal Component Analysis. (2) The ICA infomax algorithm was used to estimate independent component(s) (IC(s); Bell and Sejnowski, 1995). ICs were determined by the minimum description length (MDL) criterion (Rissanen, 1983). (3) Back reconstruction was conducted to generate time courses and spatial maps for each participant (Calhoun et al., 2009). (4) Significant IC spatial maps were thresholded using a correction for false discovery rate with a significance level of $p < 0.01$. The transformed Fisher's Z-score within the IC spatial map represented the fit (i.e., degree of correlation) of a given voxel's fMRI signal with the average fMRI signal of the IC (Greicius et al., 2007).

As graphically summarized in Fig. 2C, the component selection phase comprised four steps: (1) ICs were kept if their patterns were highly correlated with gray matter, to constrain signal changes to gray matter (Naveau et al., 2012). Spatial correlation of the IC (converted to a binary mask) with an a-priori binary mask of gray matter, white matter, and cerebrospinal fluid (using the WFU Pickatlas; Maldjian, Laurienti, Kraft and Burdette, 2003; http://fmri.wfubmgc.edu/cms/software) was calculated. ICs with high spatial correlations (top 10% of ICs) to white matter or cerebrospinal fluid as well as ICs with low spatial correlation (bottom 10% of ICs) to gray matter were dropped. (2) The Infomax ICA algorithm (Bell and Sejnowski, 1995) was conducted 20 times in ICASSO 3 to test reliability of signal decomposition (Himberg et al., 2004). Quality index (Iq) was calculated as the difference between average intra-cluster and extra-cluster similarities, reflecting compactness and isolation of a cluster that contained ICs with high similarities across runs (Himberg et al., 2004). An Iq greater than 0.8 indicated a stable ICA decomposition. (3) We also performed visual inspection and ICs were dropped if they represented eye movements, head motion, or a cardiac-induced pulsatile artifact at the brain base. (4) Finally, spatial correlation of ICs to the a-priori defined network templates provided by GIFT (Shi et al., 2018; Ye et al., 2014) were conducted with a threshold of $r > 0.1$ representing the minimum value of a small effect size (Chen et al., 2010).

For Dataset 1, the component selection process resulted in three relevant ICs: IC 4 – representing the salience network, composed of the insula, anterior cingulate cortex, and inferior frontal gyrus (Fig. 3A); IC 1 – representing the default mode network, composed of the medial prefrontal cortex, posterior cingulate cortex, precuneus, and angular gyrus (Fig. 3B); and IC 10 – representing the basal ganglia–thalamus network, composed of the pallidum, putamen, subthalamic nucleus, substantia nigra, and thalamus (Fig. 3C). The three brain networks identified in Dataset 1 were consistent with previous studies on the salience network (Uddin, 2016), the default mode network (Raichle, 2015), and the basal ganglia–thalamus network (Szewczyk-Krolikowski et al., 2014).

2.6. Statistical analyses

Hypothesis 1a. stated that chronic IN-OT modulates within-network rs-FC of the salience network, the default mode network, and the basal ganglia–thalamus network at post-intervention. To test this hypothesis, we conducted chronic IN-OT > P and chronic IN-OT < P contrasts in Dataset 1 on within-network rs-FC for the IC spatial maps of the salience network, the default mode network, and the basal ganglia–thalamus

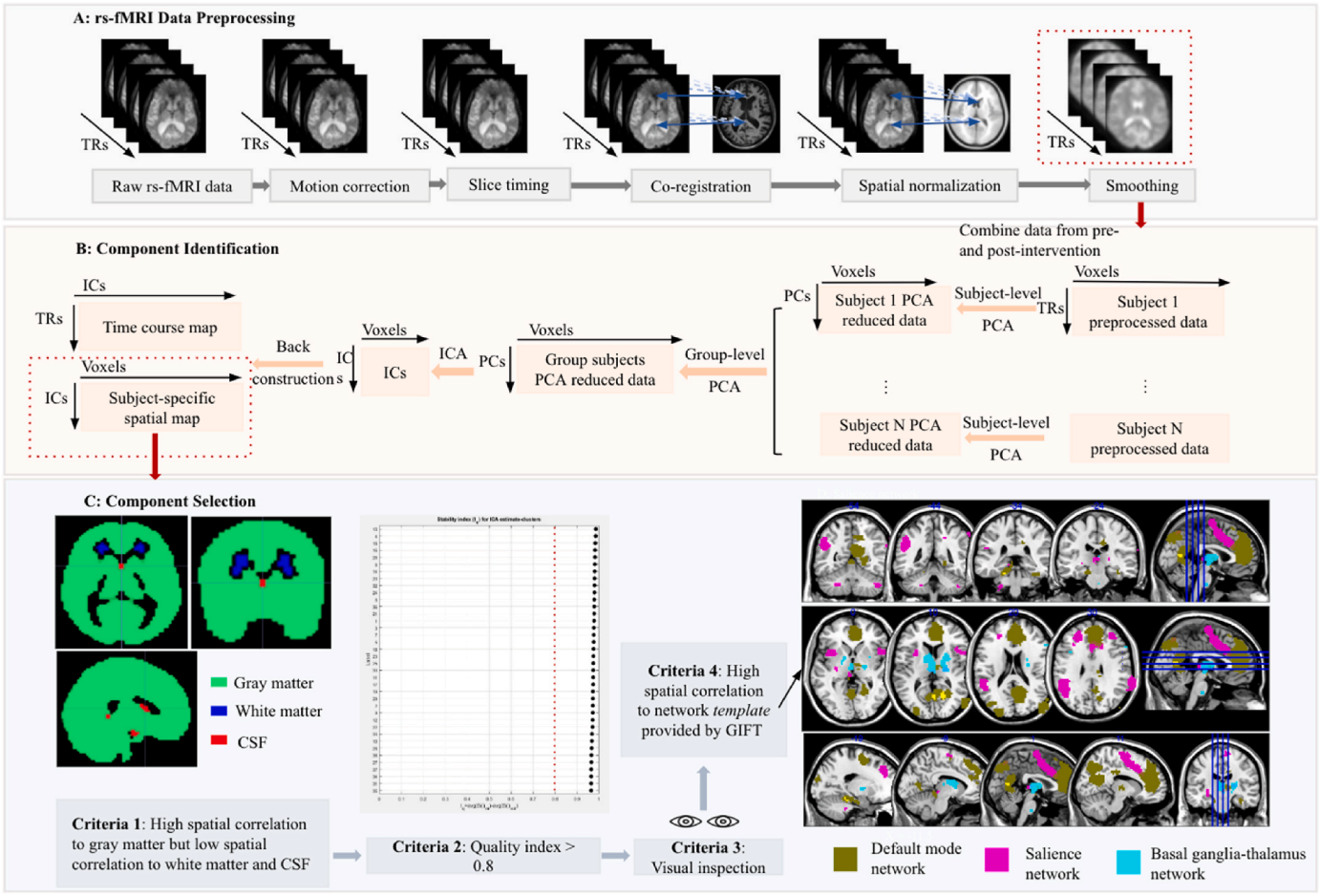

Fig. 2. Overview of Resting-State fMRI Data Preprocessing and Independent Component Analysis (ICA) Approach in Dataset 1 (Chronic IN-OT). **(A)** Resting-State fMRI Data Preprocessing: Steps including motion correction, slice timing correction, co-registration with T1 scans, spatial normalization to MNI coordinates, and smoothing using an 8 mm FWHM Gaussian kernel. **(B)** Component Identification: Four steps encompassing subject-level and group-level data dimension reduction, independent component analysis (ICA), back reconstruction for each participant, and t-tests to identify brain networks. **(C)** Component Selection: Four steps involving spatial map correlation, ICA decomposition reliability assessment, visual inspection, and correlation with brain network templates. **Abbreviations used**: TR = Time Repetition; PCA = Principal Component Analysis; PC(s) = Principal Component(s); ICA = Independent Component Analysis; ICs = Independent Component(s); CSF = Cerebrospinal Fluid.

network, respectively, as generated during the component identification process. Based on evidence that insula (peak MNI coordinates: xyz = ±30, 14, −2; Rilling et al., 2014), middle cingulate cortex (peak MNI coordinate: xyz = ±2, −12, 32; Paloyelis et al., 2016), medial prefrontal cortex (peak MNI coordinate: xyz = ±3, 47, 19; Zhao et al., 2016), and thalamus (peak MNI coordinate: xyz = ±14, 10, 4; Koch et al., 2019) constitute brain regions of IN-OT action (i.e., a-priori prediction of ROIs), we applied small volume correction to these analyses using spherical masks with a 6-mm radius around the peak voxel of these a-priori ROIs as defined by the WFU PickAtlas (Gougelet et al., 2018; Schmitz and Johnson, 2006). Additionally, we created a 6-mm radial spherical ROI ($\mathbf{ROI}_{\mathbf{brain\_region}}$) around the peak voxel of the significant brain cluster based on the contrast result to confirm that no pre-intervention differences existed between the two treatment groups (as well as for testing of Hypothesis 2a; see below). In particular, to confirm no pre-intervention treatment-group differences, we extracted and averaged the values (within-network rs-FC) of all voxels within the ROI_{brain_region} at pre-intervention and conducted Bayesian, bootstrapped independent t tests (chronic IN-OT vs. P; with 5000 resampling iterations) on the within-network rs-FC at pre-intervention.

Hypothesis 1b. stated that chronic IN-OT modulates between-network rs-FC of the salience network, the default mode network, and the basal ganglia–thalamus network at post-intervention. To test this prediction, we conducted Bayesian, bootstrapped independent t tests (chronic IN-OT vs. P; with 5000 resampling iterations) on the between-network rs-FC for each pair among these three brain networks in Dataset 1 (i.e., salience network and default mode network, salience network and basal ganglia–thalamus network, default mode network and basal ganglia–thalamus network). Between-network rs-FC was calculated as follows (Passow et al., 2015; Rubbert et al., 2019; Varangis et al., 2019): Spatial IC maps of the salience network, default mode network, and basal ganglia–thalamus network were saved as three binary-value brain network masks ($\mathbf{ROI}_{\mathbf{network}}$) respectively. Time series of each voxel from each participant were extracted within $\mathbf{ROI}_{\mathbf{network}}$. Pearson correlations were calculated for the three pairs of averaged time series of each $ROI_{network}$ to reflect the between-network rs-FC. To confirm that the two treatment groups did not differ at pre-intervention, we conducted Bayesian, bootstrapped independent t tests (chronic IN-OT vs. P; with 5000 resampling iterations) on between-network rs-FC at pre-intervention.

In exploratory fashion, we also examined effects of chronic IN-OT on specialization and efficiency of brain organization, measured via selective rs-FC between the salience network, default mode network, and basal ganglia–thalamus network, as follows (Simmons et al., 2013; Chan et al., 2014): $\textit{Selective rs-FC} = \left| \textit{rs-FC}_{(\textit{network 1, network 2})} - \textit{rs-FC}_{(\textit{network 1, network 3})} \right|$.

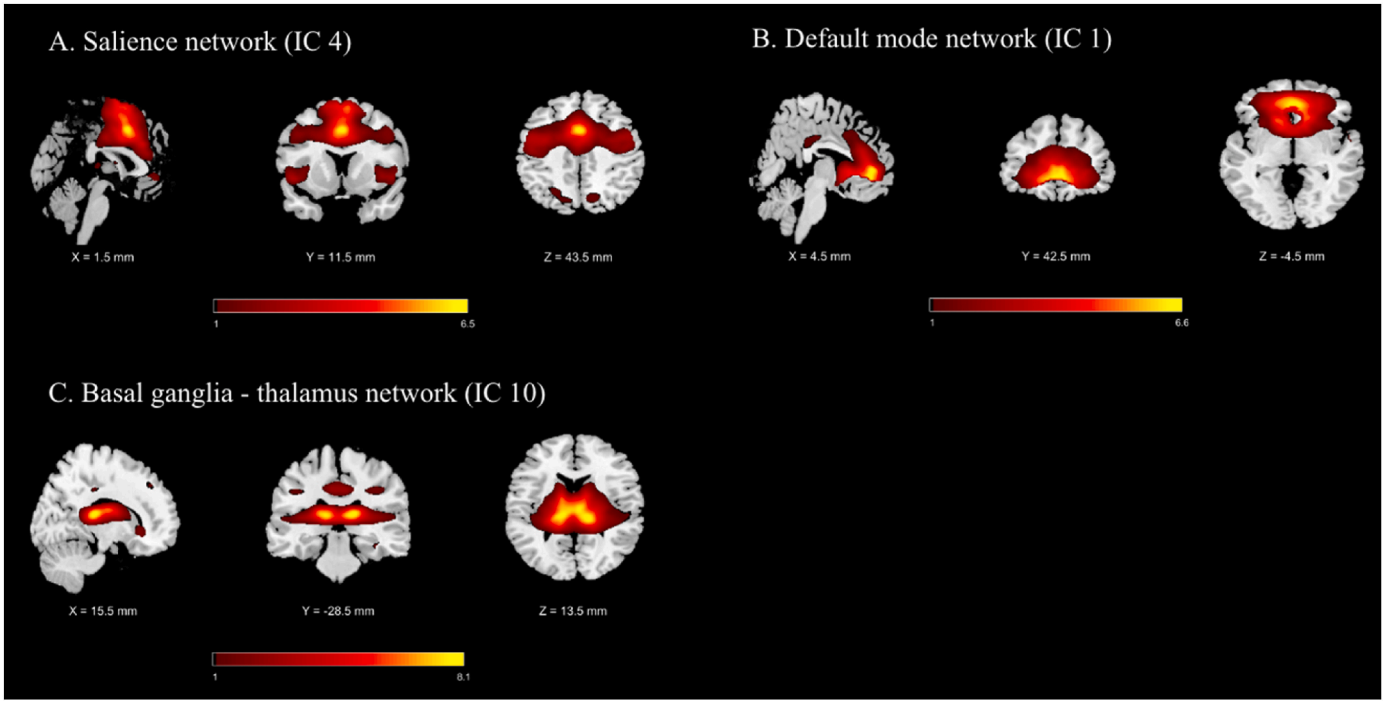

Fig. 3. Large-Scale Networks Identified in Dataset 1 (Chronic IN-OT) Using ICA. **(A)** Salience Network, **(B)** Default Mode Network, and **(C)** Basal Ganglia–Thalamus Network. Results shown on the Montreal Neurological Institute (MNI) standard brain using MNI coordinates (X, Y, Z). **Abbreviations used**: IC = Independent Component. Color bar represents t values.

Hypothesis 2a. stated that effects of chronic IN-OT on within-network rs-FC for all three networks were more pronounced than effects of acute IN-OT. To test this hypothesis, we extracted the time series of all voxels within $\mathbf{ROI_{brain\_region}}$ and $\mathbf{ROI_{network}}$ in Dataset 1 (at post-intervention) and Dataset 2, respectively. We then calculated Pearson correlations for each pair of averaged time series for each brain region ($\mathbf{ROI_{brain\_region}}$) with its corresponding brain network ($\mathbf{ROI_{network}}$), to reflect within-network rs-FC. Again, Bayesian, bootstrapped independent t tests (chronic IN-OT vs. acute IN-OT; with 5000 resampling iterations) were conducted on within-network rs-FC.

Hypothesis 2b. finally, stated that effects of chronic IN-OT on between-network rs-FC for all three networks were more pronounced than acute IN-OT effects. To test this hypothesis, we extracted the time series of all voxels within $\mathbf{ROI_{network}}$ in Dataset 1 (at post-intervention) and Dataset 2, respectively. We then calculated Pearson correlations for the three pairs of averaged time series for each $\mathbf{ROI_{network}}$, to reflect the between-network rs-FC. Again, Bayesian, bootstrapped independent t tests (chronic IN-OT vs. acute IN-OT; with 5000 resampling iterations) were conducted on between-network rs-FC.

For all models, within-network and between-network rs-FC greater or less than 3 standard deviations from the mean was regarded as outlier

and excluded from analyses. Also, all results were comparable when controlling for chronological age[2] and sex.[3]

3. Results[4]

3.1. Chronic IN-OT modulation of within-network rs-FC[5]

Chronic IN-OT relative to P resulted in reduced rs-FC of both the right insula (peak MNI coordinates: xyz = 30, 18, −6, t value = 3.37, cluster size = 14 voxels; small volume corrected *p(FWE-corrected)* = 0.013; Fig. 4A; see also Table 2) as well as the left middle cingulate cortex (peak MNI coordinates: xyz = −6, −16, 30, peak t value = 3.29, cluster size = 42 voxels; small volume corrected *p(FWE-corrected)* = 0.012; Fig. 4B) with the salience network (IC 4). Chronic IN-OT relative to P furthermore resulted in increased rs-FC of the left medial prefrontal cortex (peak MNI coordinates: xyz = −8, 48, 20, peak t value = 3.14, cluster size = 10 voxels; small volume corrected *p(FWE-corrected)* = 0.023; Fig. 4C; see also Table 2) with the default mode network (IC 1). Finally, chronic IN-OT relative to P resulted in increased rs-FC of the left thalamus (peak MNI coordinates: xyz = −14, −16, 4, peak t value = 3.14, cluster size = 9 voxels; small volume corrected *p(FWE-corrected)* = 0.024; Fig. 4D; see also Table 2) with the basal ganglia–thalamus network (IC 10). No baseline difference was found ($p > 0.05$). These results support *Hypothesis 1a* regarding OT-modulation of these three large-scale brain networks in generally healthy older adults.

3.2. Chronic IN-OT modulation of between-network rs-FC

Neither rs-FC between the salience network and the default mode network (Fisher's $Z_{\text{mean difference}} = -0.07$, bootstrapped $p = 0.41$, bootstrapped 95% confidence interval = −0.24 – 0.10, Bayesian 95% credible interval = −0.25 – 0.11, Cohen's d = −0.21; Fig. 5A), between the salience network and the basal ganglia–thalamus network (Fisher's $Z_{\text{mean difference}} = 0.10$, bootstrapped $p = 0.16$, bootstrapped 95% Confidence interval = −0.03 – 0.24, Bayesian 95% credible interval = −0.04 – 0.24, Cohen's d = 0.37; Fig. 5B), nor between the default mode network and the basal ganglia–thalamus network (Fisher's $Z_{\text{mean difference}} = -0.08$, bootstrapped $p = 0.30$, bootstrapped 95% Confidence interval = −0.06 – 0.23, Bayesian 95% credible interval = −0.08 – 0.24, Cohen's d = −0.27; Fig. 5C) were significantly different after chronic IN-OT compared to P; thus not supporting *Hypothesis 1b*. No baseline differences were found ($p > 0.05$).

Interestingly, however, selective rs-FC, as an indicator of more specialized, efficient network communication, of the basal ganglia–-thalamus network with both the salience network and the default mode network (Fisher's $Z_{\text{mean difference}} = 0.13$, bootstrapped $p = 0.02$, bootstrapped 95% confidence interval = 0.02–0.23, Bayesian 95% credible interval = 0.02–0.24, Cohen's d = 0.61; Fig. 5F) was significantly increased for chronic IN-OT relative to P. In contrast, neither selective rs-FC of the salience network with the default mode and the basal ganglia–thalamus network (Fisher's $Z_{\text{mean difference}} = 0.03$, bootstrapped $p = 0.63$, bootstrapped 95% confidence interval = 0.09–0.15, Bayesian 95% credible interval = −0.09 – 0.15, Cohen's d = 0.12; Fig. 5D) nor selective rs-FC of the default mode network with the salience network and the basal ganglia–thalamus network (Fisher's $Z_{\text{mean difference}} = 0.003$, bootstrapped $p = 0.96$, bootstrapped 95% confidence interval = −0.12 – 0.11, Bayesian 95% credible interval = −0.12 – 0.13, Cohen's d = 0.02) were significant (see Fig. 5E). No baseline differences were found ($p > 0.05$).

3.3. Comparison of chronic and acute IN-OT effects on within- and between-network rs-FC

Regarding within-network connectivity, chronic compared to acute IN-OT resulted in a greater reduction of rs-FC of the right insula with the salience network (Fisher's $Z_{\text{mean difference}} = -0.49$, t (1,48) = −4.36, bootstrapped $p < 0.001$, bootstrapped 95% confidence interval = 0.30–0.70, Bayesian 95% credible interval = 0.27–0.70, Cohen's d = −1.26; Fig. 6A; see Fig. S4 in the Supplementary Materials for details), in support of *Hypothesis 2a*. However, rs-FC of the left middle cingulate cortex with the salience network (Fisher's $Z_{\text{mean difference}} = -0.06$, bootstrapped $p = 0.65$, bootstrapped 95% confidence interval = −0.28 – 0.19, Bayesian 95% credible interval = −0.30 – 0.19, Cohen's d = −0.12), the left medial prefrontal cortex with the default mode network (Fisher's $Z_{\text{mean difference}} = -0.23$, bootstrapped $p = 0.06$, bootstrapped 95% confidence interval = −0.47 – 0.01, Bayesian 95% credible interval = −0.45 – 0.00, Cohen's d = −0.55), or the left thalamus with the basal ganglia–thalamus network (Fisher's $Z_{\text{mean difference}} = -0.25$, bootstrapped $p = 0.07$, bootstrapped 95% confidence interval = −0.52 – 0.02, Bayesian 95% credible interval = −0.49 – 0.00, Cohen's d = −0.54) were not different for chronic and acute IN-OT.

Regarding between-network connectivity, chronic compared to acute IN-OT resulted in more reduced rs-FC between the default mode network and the basal ganglia–thalamus network (Fisher's $Z_{\text{mean difference}} = -0.48$, bootstrapped $p < 0.001$, bootstrapped 95% confidence interval = −0.65 to −0.30, Bayesian 95% credible interval = −0.66 to −0.30, Cohen's d = −1.50; Fig. 6B), in support of *Hypothesis 2b*.

[2] Given the wide chronological age range in our sample, we conducted parallel analyses to the ones reported in-text with chronological age as a moderator. These results showed no significant interaction of chronological age by treatment on any of the within-network rs-FC analyses (i.e., right insula with the salience network (F (1, 55) = 0.80, $p = 0.38$), left middle cingulate cortex with the salience network (F (1, 55) = 0.39, $p = 0.54$), left medial prefrontal cortex with the default mode network (F (1, 55) = 3.62, $p = 0.06$), or left thalamus with the basal ganglia–thalamus network (F (1, 55) = 0.72, $p = 0.40$)); any of the between-network rs-FC analyses (i.e., salience network and default mode network (F (1, 56) = 0.07, $p = 0.80$), salience network and basal ganglia–thalamus network (F (1, 56) = 0.07, $p = 0.80$), or default mode network and basal ganglia–thalamus network (F (1, 56) = 0.00, $p = 0.97$)); nor any of the selective rs-FC analyses on the salience network (F (1, 56) = 1.25, $p = 0.27$), the default mode network (F (1, 56) = 0.05, $p = 0.82$), and the basal–ganglia thalamus network (F (1, 56) = 0.09, $p = 0.77$). See also Fig. S1 in the Supplementary Materials.

[3] We also considered sex as a moderator based on evidence in the literature of sex-dimorphic functions of IN-OT on the brain (Reed et al., 2019; Rilling et al., 2014), including among older adults (Ebner et al., 2016). The 2 treatment group (chronic IN-OT, P) by 2 timepoint (pre-intervention, post-intervention) by sex (male, female) interaction was not significant for (i) any of the within-network rs-FC analyses (i.e., right insula with the salience network (F (1, 56) = 1.19, p = 0.28), left middle cingulate cortex with the salience network (F (1, 56) = 0.23, p = 0.88), left medial prefrontal cortex with the default mode network (F (1, 56) = 0.16, p = 0.70), or left thalamus with the basal ganglia–thalamus network (F (1, 56) = 0.06, p = 0.80)); (ii) any of the between-network rs-FC analyses (i.e., salience network and default mode network (F (1, 56) = 0.001, p = 0.97), salience network and basal ganglia–-thalamus network (F (1, 56) = 0.81, p = 0.37), or default mode network and basal ganglia–thalamus network (F (1, 56) = 0.13, p = 0.73)); nor (iii) any of the selective rs-FC analyses on the salience network (F (1, 56) = 0.52, p = 0.48), the default mode network (F (1, 56) = 0.04, p = 0.84), or the basal–ganglia thalamus network (F (1, 56) = 1.62, p = 0.21). See Figs. S2 and S3 in the Supplementary Materials for details.

[4] Results for Hypotheses 1 b, 2a & 2 b remained the same when applying Bonferroni correction (Hypothesis 1b: adj. p = 0.05/3 = 0.017; Hypothesis 2a: adj. p = 0.05/4 = 0.013; Hypothesis 2b: adj. p = 0.05/3 = 0.017).

[5] Note that an equivalent analysis was conducted in Liu et al. (2022) on Dataset 2. However, in that paper we focused on the salience network as the primary brain network under investigation (and the default mode network as a secondary) and on effects of acute IN-OT. Crucially extending this previous work, the current paper included the basal ganglia–thalamus network as well as conducted between-network analysis in addition to within-network analysis. Furthermore, the present paper directly compared chronic and acute IN-OT effects on large-scale brain network connectivity at rest, and important extension not previously covered.

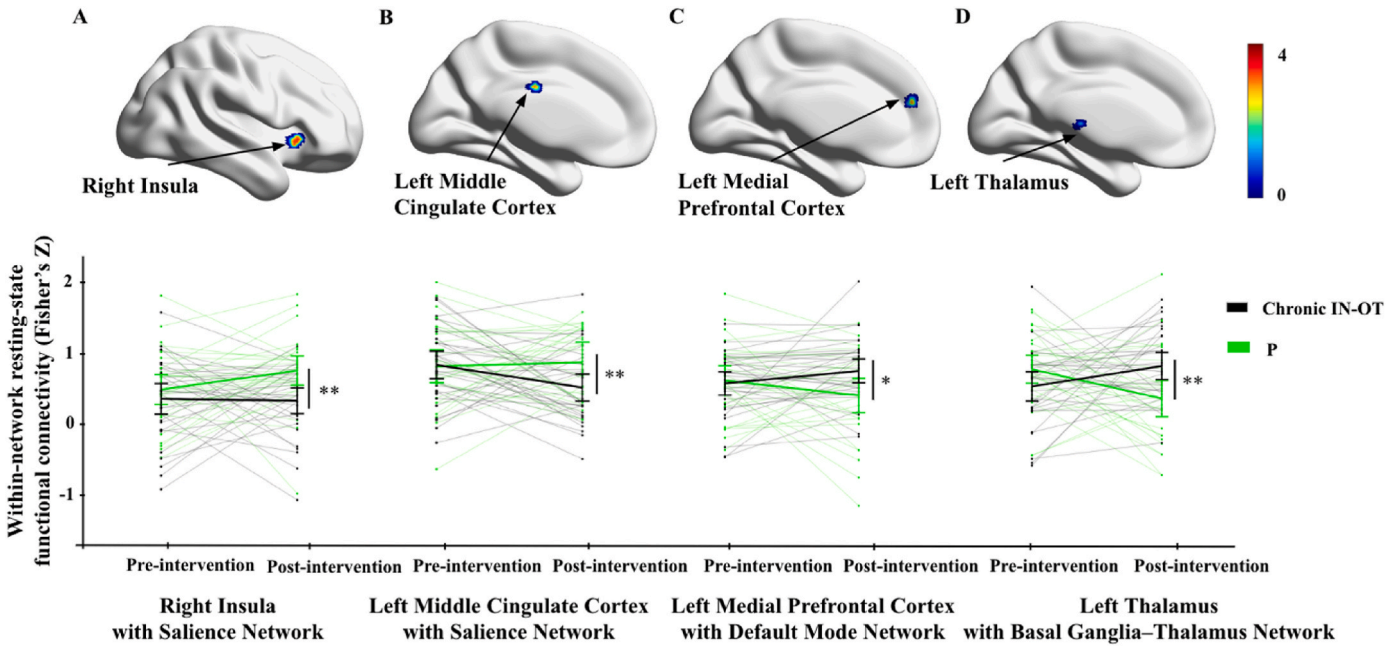

Fig. 4. Effects of Chronic IN-OT on Within-Network rs-FC in Dataset 1. **(A)** Right Insula with Salience Network; **(B)** Left Middle Cingulate Cortex with Salience Network; **(C)** Left Medial Prefrontal Cortex with Default Mode Network; and **(D)** Left Thalamus with Basal Ganglia–Thalamus Network. For better display quality and data population distribution results are shown at $p < 0.01$ (uncorrected). Dots represent individual participants; lines connect each individual participant's data at pre- and post-intervention, with a positive slope indicating increase and a negative slope indicating decrease in rs-FC from pre-to post-intervention. **Abbreviations used**: IN-OT = Intranasal Oxytocin (in black); P = Placebo (in green). Error bar indicates 95% confidence interval. * indicates uncorrected $p < 0.05$; ** indicates uncorrected $p < 0.01$. Spectral color bar represents t-values.

Table 2
Treatment Group (Chronic IN-OT vs. P) x Timepoint (Pre-vs. Post-Intervention) ANOVAs on Within-Network rs-FC in Three Large-Scale Brain Networks in Dataset 1.

Brain networks	MNI (x,y, z)	T value	Cluster size	Corrected *p* value
Salience network (IC 4)				
Chronic IN-OT < P				
Right insula	30, 18, −6	3.37	14	0.013
Left middle cingulate cortex	−6, −16, 30	3.29	42	0.012
Chronic IN-OT > P				ns
Default mode network (IC 1)				
Chronic IN-OT < P				ns
Chronic IN-OT > P				
Left medial prefrontal cortex	−8, 48, 20	3.14	10	0.023
Basal ganglia–thalamus network (IC 10)				
Chronic IN-OT < P				ns
Chronic IN-OT > P				
Left thalamus	−14, −16, 4	3.14	9	0.024

Note: Each region underwent small volume correction with a peak-level threshold of *p(FWE-corrected)* < 0.05. ns indicates not significant.

However, rs-FC between the salience network and the basal ganglia–thalamus network (Fisher's $Z_{mean\ difference} = 0.001$, bootstrapped $p = 0.99$, bootstrapped 95% confidence interval = −0.17– 0.18, Bayesian 95% credible interval = −0.18 – 0.18, Cohen's d = 0.01) and between the salience network and the default mode network (Fisher's $Z_{mean\ difference} = 0.10$, bootstrapped $p = 0.32$, bootstrapped 95% confidence interval = −0.30– 0.10, Bayesian 95% credible interval = −0.31 – 0.11, Cohen's d = 0.29*)* were not different for chronic and acute IN-OT.

Finally, chronic compared to acute IN-OT resulted in greater selective rs-FC of the salience network with both the default mode network and the basal ganglia–thalamus network (Fisher's $Z_{mean\ difference} = 0.13$, bootstrapped $p = 0.01$, bootstrapped 95% confidence interval = 0.04–0.23, Bayesian 95% credible interval = 0.03–0.23, Cohen's d = 0.67; Fig. 6C). However, selective rs-FC of the default mode network with the salience network and the basal ganglia–thalamus network (Fisher's $Z_{mean\ difference} = 0.06$, bootstrapped $p = 0.27$, bootstrapped 95% confidence interval = −0.05 – 0.17, Bayesian 95% credible interval = −0.17 – 0.05, Cohen's d = 0.30) as well as the basal ganglia–thalamus network with the salience network and the default mode network (Fisher's $Z_{mean\ difference} = 0.08$, bootstrapped $p = 0.18$, bootstrapped 95% Confidence interval = −0.04 – 0.20, Bayesian 95% credible interval = −0.04 – 0.20, Cohen's d = 0.39) were not different for chronic and acute IN-OT (see Fig. S5 in the Supplementary Materials for details).

4. Discussion

Taking a large-scale network approach, the present study investigated the effects of chronic IN-OT on both within- and between-network rs-FC of the salience network, the default mode network, and the basal ganglia–thalamus network in a sample of generally healthy older adults. The main findings revealed significant alterations in rs-FC within these three networks following chronic IN-OT. In addition, chronic IN-OT (relative to P) resulted in significantly greater selective rs-FC of the basal ganglia–thalamus network with both the salience network and the default mode network, highlighting higher specialization, modularity, and efficiency of coupling between these networks following chronic IN-OT. Directly comparing chronic with acute IN-OT, we furthermore observed more pronounced IN-OT effects on both within- and between-network rf-FC following chronic than acute IN-OT. These various novel findings and their implications are discussed next.

4.1. Chronic IN-OT modulated within-network rs-FC in three large-scale brain networks in older adults

4.1.1. Chronic IN-OT reduced rs-FC within the salience network

Chronic IN-OT resulted in reduced rs-FC of the right insula with the

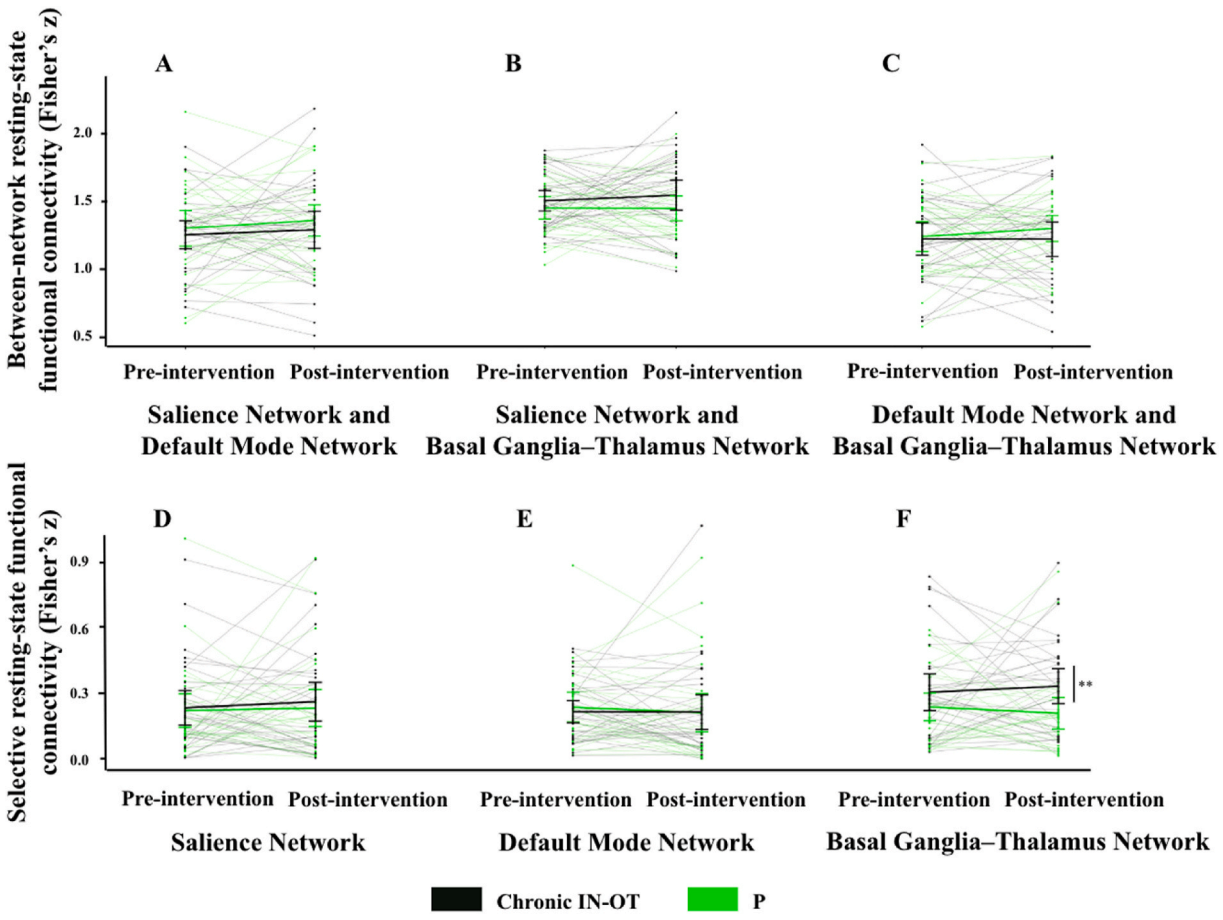

Fig. 5. Effects of Chronic IN-OT on Between-Network rs-FC and on Selective rs-FC, respectively. Between-Network rs-FC for **(A)** Salience Network and Default Mode Network; **(B)** Salience Network and Basal Ganglia–Thalamus Network; **(C)** Default Mode Network and Basal Ganglia–Thalamus Network. Selective rs-FC of **(D)** Salience Network; **(E)** Default Mode Network; **(F)** Basal Ganglia–Thalamus Network with the other two brain networks, respectively. For better display quality and data population distribution results are shown at $p < 0.01$ (uncorrected). Dots represent individual participants; lines connect each individual participant's data at pre- and post-intervention, with a positive slope indicating increase and a negative slope indicating decrease in rs-FC from pre-to post-intervention. **Abbreviations used**: IN-OT = Intranasal Oxytocin (in black); P = Placebo (in green). Error bar indicates 95% confidence interval. ** indicates uncorrected $p < 0.01$.

salience network in older adults. This finding may reflect OT-modulation of cognitive-emotional information processing within the salience network (Menon, 2015) and is closely aligned with results reported by Liu et al. (2022) regarding acute IN-OT, which showed decreased rs-FC of the right insula with the salience network in a sample comprising both younger and older adults. Insula plays a crucial role in bottom-up processing of novel and salient stimuli, particularly for negative emotional stimuli (e.g., related to anxiety, fear, uncertainty; Ince et al., 2023; Menon and Uddin, 2010). Our findings of reduced rs-FC of the insula with the salience network therefore could signify a regulatory effect of OT on transmission of emotional information within the salience network.

Chronic IN-OT also resulted in reduced rs-FC of the left middle cingulate cortex with the salience network. Middle cingulate cortex is involved in the processing of reward-related information, conflict detection, and error monitoring (Hu et al., 2013; Rolls, 2019). Chronic IN-OT-reduced connectivity of the middle cingulate cortex with the salience network may be reflective of a mechanism through which OT modulates sensitivity to reward-related stimuli, which could underlie the neuropeptide's role in promoting prosocial behavior by redirecting individuals towards a more altruistic orientation (Jones et al., 2017).

4.1.2. Chronic IN-OT increased rs-FC within the default mode network in older adults

In contrast, chronic IN-OT increased rs-FC between the left medial prefrontal cortex with the default mode network in older adults, supporting the role of OT in social cognition (Raichle, 2015; Schilbach et al., 2008) as well as the integration of emotional and cognitive processes such as in the context of empathy, theory of mind, and moral judgments (Li and Rieckmann, 2014). This finding is in line with previous evidence of acute IN-OT enhancing rs-FC of the medial prefrontal cortex with subcortical regions, such as the amygdala (Ebner et al., 2016; Sripada et al., 2013) in both young and older adults.

4.1.3. Chronic IN-OT increased rs-FC within the basal Ganglia–Thalamus network in older adults

We also found that chronic IN-OT increased rs-FC of the left thalamus with the basal ganglia–thalamus network in older adults. The basal ganglia–thalamus network is crucial for reward-related information processing, and the thalamus plays a critical role in emotional up-regulation through cognitive reappraisal (Koch et al., 2019; Wager et al., 2008). Chronic IN-OT increased coupling within the basal ganglia–thalamus network may represent a neural mechanism underlying OT's role in emotion regulation (Koch et al., 2019).

In sum, the pattern of results observed here for chronic IN-OT modulation of within-network rs-FC within the salience network, the default mode network, and the basal ganglia–thalamus network combined suggest that OT may act through mitigating down-regulation ("bottom-up") of emotion processing areas (i.e., insula and middle cingulate cortex within the salience network), as well as enhancing up-

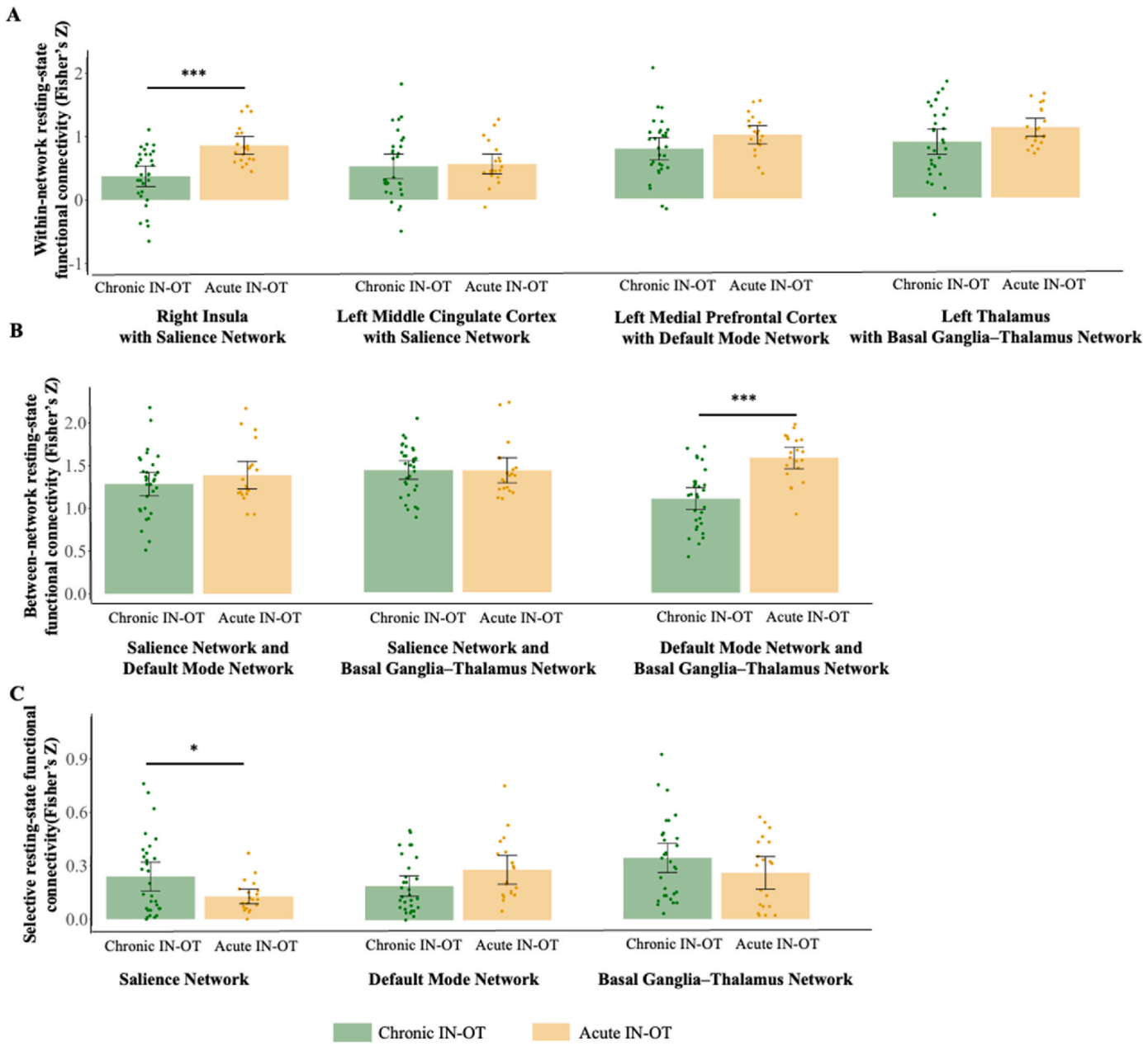

Fig. 6. Comparison between Chronic vs. Acute IN-OT on **(A)** Within-Network rs-FC, **(B)** Between-Network rs-FC, and **(C)** Selective rs-FC between Salience Network, Default Mode Network, and Basal Ganglia–Thalamus Network. Dots represent individual participants. rs-FC = resting-state functional connectivity. **Abbreviations used**: IN-OT = Intranasal Oxytocin. Error bars indicate 95% confidence interval. * indicates uncorrected $p < 0.05$; *** indicates uncorrected $p < 0.001$.

regulation ("top-down") of emotional control areas (i.e., medial prefrontal cortex within the default mode network and thalamus within the basal ganglia–thalamus network). Overall, our findings provide first compelling evidence of an impact of chronic IN-OT effects on within large-scale brain network connectivity in older adults, shedding light on the neural mechanisms of OT in aging via brain network functional connectivity with relevance to emotion and social cognition.

4.2. Chronic IN-OT modulated selective rs-FC of the basal Ganglia–Thalamus network with the salience network and the default mode network

We did not observe modulation of chronic IN-OT on between-network modulation of rs-FC between the salience network, the default mode network, and the basal ganglia–thalamus network in older adults; in contrast to our predictions, which were based on the few acute IN-OT studies that examined between-network connectivity (Bethlehem et al., 2017; Brodmann et al., 2017; Zheng et al., 2021). These previous studies, however, exclusively comprised young adults. Young and older adults often exhibit distinct brain functional patterns (Geerligs et al., 2015), including regarding resting-state coupling (Chen et al., 2017; Farras-Permanyer et al., 2019; Mary et al., 2017).

However, when examining functional coupling between these three large-scale brain networks via the novel measure of *selective rs-FC*, which reflects efficiency of communication between brain networks (Simmons et al., 2013; Chan et al., 2014), we observed increased selective coupling of the basal ganglia–thalamus network with the salience network and the default mode network after chronic IN-OT relative to P in older adults (while there were no effects on the other two brain networks). This qualification of our results indicates that chronic IN-OT may selectively influence functional connectivity patterns, aligning with the concept of modular organization, where specific modules or

communities exhibit varying levels of connectivity and interaction with other modules (Chan et al., 2014). In fact, the basal ganglia–thalamus network's differential connectivity with the default mode network and the salience network after chronic IN-OT we observed may reflect OT's unique role in coordinating "down-regulation" (via the salience network) while "up-regulation" (via the default mode network) of emotional/salient information. By investigating selective rs-FC for the first time in the context of IN-OT research and in older adults, this study importantly advances understanding of the OT's effects on specificity and efficiency of brain network interactions.

Unlike conventional approaches that may overlook subtle alterations in network interactions, measuring selective rs-FC allows for a more nuanced exploration of connectivity changes among brain networks, given the distinctive nature of selective rs-FC, which estimates relationships across multiple brain networks rather than focusing solely on specific pairs (Chan et al., 2014; Power et al., 2011; Simmons et al., 2013). This more integrative approach enhances sensitivity to capture intricacies of network dynamics influenced by IN-OT.

4.3. More pronounced effects of chronic compared to acute IN-OT on within- and between-network rs-FC in older adults

Directly compared to acute IN-OT, chronic IN-OT resulted in a more pronounced reduction in rs-FC of the right insula with the salience network, more pronounced reduced rs-FC of the default mode network with the basal ganglia–thalamus network, and relatively greater selective rs-FC of the salience network with both the default mode and the basal ganglia–thalamus network. Current knowledge on chronic IN-OT on brain and behavior in older adults is still limited (Horta et al., 2020; Valdes-Hernandez et al., 2021), and our study is the first to directly compare the magnitudes of chronic and acute IN-OT effects on brain network connectivity in older adults. Acute administration tends to evoke immediate, transient effects, whereas chronic administration potentially triggers prolonged alterations in brain networks (Horta et al., 2020). Taken together, our findings support the notion that chronic IN-OT induces more pronounced brain mechanistic effects and thus may bear greater therapeutic potential in older adults than a single-dose acute administration.

Our findings of more pronounced chronic than acute IN-OT effects underscore potential advantages associated with prolonged exposure to IN-OT. Peters et al. (2014) have indicated that chronic IN-OT regimens allow for sustained exposure to OT, amplifying its influence on neural systems. Prolonged exposure may contribute to increased receptor sensitivity (Zanos et al., 2014). Additionally, neuroplastic changes associated with chronic IN-OT could play a pivotal role in enhancing OT's effects on the brain (e.g., rs-FC) and behavior. Chronic IN-OT is linked to a decrease in epigenetic methylation of the OT receptor, accompanied by an increase in OT receptor expression (Alaerts et al., 2023; Moerkerke et al., 2024). These neuroplastic alterations may create a conducive neural environment for OT to exert its modulatory effects on functional connectivity within and between large-scale brain networks.

IN-OT has previously shown therapeutic potential in posttraumatic stress disorder (Giovanna et al., 2020; Matsushita et al., 2019; Sippel et al., 2017), autism (Watanabe et al., 2015; Yamasue, 2016), and fear disorders (Baldi et al., 2021). Our study demonstrated that chronic IN-OT modulates large-scale network rs-FC among older adults, further informing OT's brain mechanism of action in treatment. Future research could test IN-OT in combination with behavioral and cognitive training (Cao et al., 2016; Han et al., 2017; Sun et al., 2020) or targeted brain modulation such as via Transcranial Magnetic Stimulation (TMS; Luber and Lisanby, 2014) in to develop most effective therapy.

4.4. Limitations

The present study is making several significant novel contributions regarding OT's role in modulating within and between large-scale neural network communication. However, some limitations should be acknowledged. First, our sample consisted exclusively of older adults, limiting the study's ability to directly speak to aging effects or generalizability to other age groups. Future studies should explore chronic IN-OT effects on brain network connectivity in more diverse populations (including middle-aged adults, older adults with a history of adversity, clinical aging populations), also to allow determination of moderating effects in the observed relationships. Second, our study focused on IN-OT modulation of rs-FC (i.e., task-free), but investigation of associations between brain connectivity patterns and specific social-cognitive and/or behavioral outcomes is crucial (see Fig. S6 in the Supplementary Material for an association between brain connectivity and apathy in our sample). Third, our study did not reveal sex differences, perhaps due to the small sample size which was not adequately powered to detect significant sex moderations. Future investigations should employ larger sample sizes with equal representation of women and men given evidence of sex-dimorphic effects of IN-OT on brain and behavior among older adults (Horta et al., 2020).

Finally, moving forward analysis of structural connectivity (e.g., structural diffusion tensor imaging derived connectivity measures) contributing to the functional connectivity patterns observed in our study could provide valuable insights into the impact of chronic IN-OT on the aging brain.

5. Conclusions

In sum, findings from our study support a modulatory role of chronic IN-OT on within-network functional coupling of the salience network, the default mode network, and the basal ganglia–thalamus network in older adults, as well as effects on selective rs-FC among these networks. Moreover, we demonstrate for the first time that chronic compared to acute IN-OT produces more pronounced effects on brain network connectivity, underscoring the importance of duration and frequency in administration regimens to unfold IN-OT's full treatment potential on brain and behavior among older adults.

CRediT authorship contribution statement

Peiwei Liu: Writing – review & editing, Writing – original draft, Visualization, Validation, Methodology, Formal analysis, Conceptualization. **Tian Lin:** Writing – review & editing, Methodology, Conceptualization. **Håkan Fischer:** Writing – review & editing, Methodology, Conceptualization. **David Feifel:** Writing – review & editing, Resources, Methodology, Data curation. **Natalie C. Ebner:** Writing – review & editing, Visualization, Validation, Supervision, Software, Resources, Project administration, Methodology, Investigation, Funding acquisition, Formal analysis, Data curation, Conceptualization.

Declaration of competing interest

The authors declare that they have no known competing financial interests or personal relationships that could have appeared to influence the work reported in this paper.

Data availability

Data will be made available on request.

Acknowledgments

This work was supported by the Scientific Research Network on Decision Neuroscience and Aging pilot award (R24 AG039350); the National Institute on Aging grants (R01AG059809); the National Institute on Drug Abuse grant (R21DA056813); the US Navy Office of Naval Research (N00014-21-1-2201); the University of Florida (UF) Clinical and Translational Science pilot award (NIH/NCATS, UL1 TR000064);

the UF Pain Research and Intervention Center of Excellence-Clinical and Translational Science Institute-Institute on Aging grant (ARG DTD 03-26-2008); the UF College of Liberal Arts and Sciences; the UF Psychology Department; the UF Center for Cognitive Aging and Memory; the UF Claude D. Pepper Older Americans Independence Center (P30AG028740); the UF Jacquelin Spring Fellowship; the UF Jacquelin Research Grant Award; the Jacquelin Goldman Dissertation Award; and the Charles Vincent and Heidi Cole McLaughlin CLAS Dissertation Fellowship. A portion of this work was performed in the McKnight Brain Institute at the National High Magnetic Field Laboratory's AMRIS Facility, supported by National Science Foundation Cooperative Agreement No. DMR-1157490 and the State of Florida. Spray bottles were provided by SGD Pharma and spray pumps were provided by Aptar Pharma.

The content of this paper is solely the responsibility of the author(s) and does not necessarily represent the official views of the National Institutes of Health.

Appendix A. Supplementary data

Supplementary data to this article can be found online at https://doi.org/10.1016/j.neuropharm.2024.110130.

References

Akshoomoff, N., et al., 2013. VIII. NIH ToolboxCognition Battery (CB): composite scores ofcrystallized, fluid, and overall cognition. Monogr. Soc. Res. Child Dev. 78, 119–132. https://doi.org/10.1111/MONO.12038.

Alaerts, K., Daniels, N., Moerkerke, M., Evenepoel, M., Tang, T., Van der Donck, S., Chubar, V., Claes, S., Steyaert, J., Boets, B., 2023. At the head and heart of oxytocin: an RCT investigating stress-regulatory neural and cardiac effects of chronic administration in children with autism. medRxiv 2004–2023.

Andrews-Hanna, J.R., Smallwood, J., Spreng, R.N., 2014. The default network and self-generated thought: component processes, dynamic control, and clinical relevance. Ann. N. Y. Acad. Sci. 1316 (1), 29–52.

Baldi, E., Costa, A., Rani, B., Passani, M.B., Blandina, P., Romano, A., Provensi, G., 2021. Oxytocin and fear memory extinction: possible implications for the therapy of fear disorders? Int. J. Mol. Sci. 22 (18), 10000.

Bell, A.J., Sejnowski, T.J., 1995. An information-maximization approach to blind separation and blind deconvolution. Neural Comput. 7 (6), 1129–1159.

Bellec, P., Perlbarg, V., Jbabdi, S., Pélégrini-Issac, M., Anton, J.L., Doyon, J., Benali, H., 2006. Identification of large-scale networks in the brain using fMRI. Neuroimage 29 (4), 1231–1243.

Bethlehem, R.A.I., Lombardo, M.V., Lai, M.C., Auyeung, B., Crockford, S.K., Deakin, J., Soubramanian, S., Sule, A., Kundu, P., Voon, V., Baron-Cohen, S., 2017. Intranasal oxytocin enhances intrinsic corticostriatal functional connectivity in women. Transl. Psychiatry. https://doi.org/10.1038/tp.2017.72.

Brusa, L., Petta, F., Pisani, A., Moschella, V., Iani, C., Stanzione, P., et al., 2007. Acute vs chronic effects of l-dopa on bladder function in patients with mild Parkinson disease. Neurology 68 (18), 1455–1459.

Brodmann, K., Gruber, O., Goya-Maldonado, R., 2017. Intranasal oxytocin selectively modulates large-scale brain networks in humans. Brain Connect. https://doi.org/10.1089/brain.2017.0528.

Burmester, V., Higgs, S., Terry, P., 2018. Rapid-onset anorectic effects of intranasal oxytocin in young men. Appetite 130, 104–109.

Cabral, J., Hugues, E., Sporns, O., Deco, G., 2011. Role of local network oscillations in resting-state functional connectivity. Neuroimage 57 (1), 130–139.

Calhoun, V.D., Liu, J., Adalı, T., 2009. A review of group ICA for fMRI data and ICA for joint inference of imaging, genetic, and ERP data. Neuroimage 45 (1), S163–S172.

Campbell, I., 2007. Chi-squared and Fisher–Irwin tests of two-by-two tables with small sample recommendations. Stat. Med. 26 (19), 3661–3675.

Cao, W., Cao, X., Hou, C., Li, T., Cheng, Y., Jiang, L., et al., 2016. Effects of cognitive training on resting-state functional connectivity of default mode, salience, and central executive networks. Front. Aging Neurosci. 8, 70.

Chan, M.Y., Park, D.C., Savalia, N.K., Petersen, S.E., Wig, G.S., 2014. Decreased segregation of brain systems across the healthy adult lifespan. Proc. Natl. Acad. Sci. USA 111 (46), E4997–E5006.

Chen, H., Cohen, P., Chen, S., 2010. How big is a big odds ratio? Interpreting the magnitudes of odds ratios in epidemiological studies. Commun. Stat. Simulat. Comput. 39 (4), 860–864.

Chen, Y., Wang, W., Zhao, X., Sha, M., Liu, Y., Zhang, X., Ma, J., Ni, H., Ming, D., 2017. Age-related decline in the variation of dynamic functional connectivity: a resting state analysis. Front. Aging Neurosci. 9, 203.

De Cagna, F., Fusar-Poli, L., Damiani, S., Rocchetti, M., Giovanna, G., Mori, A., Politi, P., Brondino, N., 2019. The role of intranasal oxytocin in anxiety and depressive disorders: a systematic review of randomized controlled trials. Clinical Psychopharmacology and Neuroscience 17 (1), 1.

Di Simplicio, M., Massey-Chase, R., Cowen, P.J., Harmer, C.J., 2009. Oxytocin enhances processing of positive versus negative emotional information in healthy male volunteers. J. Psychopharmacol. 23 (3), 241–248.

Ebner, N.C., Chen, H., Porges, E., Lin, T., Fischer, H., Feifel, D., Cohen, R.A., 2016. Oxytocin's effect on resting-state functional connectivity varies by age and sex. Psychoneuroendocrinology. https://doi.org/10.1016/j.psyneuen.2016.03.013.

Ebner, N.C., Maura, G.M., MacDonald, K., Westberg, L., Fischer, H., 2013. Oxytocin and socioemotional aging: current knowledge and future trends. Front. Hum. Neurosci. https://doi.org/10.3389/fnhum.2013.00487.

Frazier, I., Lin, T., Liu, P., Skarsten, S., Feifel, D., Ebner, N.C., 2021. Age and intranasal oxytocin effects on trust-related decisions after breach of trust: behavioral and brain evidence. Psychol. Aging 36 (1), 10.

Farras-Permanyer, L., Mancho-Fora, N., Montalà-Flaquer, M., Bartrés-Faz, D., Vaqué-Alcázar, L., Peró-Cebollero, M., Guàrdia-Olmos, J., 2019. Age-related changes in resting-state functional connectivity in older adults. Neural Regeneration Research 14 (9), 1544.

Geerligs, L., Renken, R.J., Saliasi, E., Maurits, N.M., Lorist, M.M., 2015. A brain-wide study of age-related changes in functional connectivity. Cerebr. Cortex. https://doi.org/10.1093/cercor/bhu012.

Giovanna, G., Damiani, S., Fusar-Poli, L., Rocchetti, M., Brondino, N., de Cagna, F., et al., 2020. Intranasal oxytocin as a potential therapeutic strategy in post-traumatic stress disorder: a systematic review. Psychoneuroendocrinology 115, 104605.

Gougelet, R., Terzibas, C., Voytek, B., Callan, D., 2018. Functional network activity mediating the shift of attentional resources during inattentional deafness in an aviation pursuit task. Front. Hum. Neurosci. https://doi.org/10.3389/conf.fnhum.2018.227.00117.

Greicius, M.D., Flores, B.H., Menon, V., Glover, G.H., Solvason, H.B., Kenna, H., et al., 2007. Resting-state functional connectivity in major depression: abnormally increased contributions from subgenual cingulate cortex and thalamus. Biol. Psychiatr. 62 (5), 429–437.

Grimm, S., Boesiger, P., Beck, J., Schuepbach, D., Bermpohl, F., Walter, M., Ernst, J., Hell, D., Boeker, H., Northoff, G., 2009. Altered negative BOLD responses in the default-mode network during emotion processing in depressed subjects. Neuropsychopharmacology 34 (4), 932–943.

Guastella, A.J., Hickie, I.B., McGuinness, M.M., Otis, M., Woods, E.A., Disinger, H.M., et al., 2013. Recommendations for the standardisation of oxytocin nasal administration and guidelines for its reporting in human research. Psychoneuroendocrinology 38 (5), 612–625.

Haber, S.N., Calzavara, R., 2009. The cortico-basal ganglia integrative network:s the role of the thalamus. Brain Res. Bull. 78 (2–3), 69–74.

Han, K., Davis, R.A., Chapman, S.B., Krawczyk, D.C., 2017. Strategy-based reasoning training modulates cortical thickness and resting-state functional connectivity in adults with chronic traumatic brain injury. Brain and Behavior 7 (5), e00687.

Himberg, J., Hyvärinen, A., Esposito, F., 2004. Validating the independent components of neuroimaging time series via clustering and visualization. Neuroimage 22 (3), 1214–1222.

Horta, M., Kaylor, K., Feifel, D., Ebner, N.C., 2020a. Chronic oxytocin administration as a tool for investigation and treatment: a cross-disciplinary systematic review. In: Neuroscience and Biobehavioral Reviews. https://doi.org/10.1016/j.neubiorev.2019.10.012.

Horta, M., Pehlivanoglu, D., Ebner, N.C., 2020b. The role of intranasal oxytocin on social cognition: an integrative human lifespan approach. In: Current Behavioral Neuroscience Reports. https://doi.org/10.1007/s40473-020-00214-5.

Horta, M., Ziaei, M., Lin, T., Porges, E.C., Fischer, H., Feifel, D., et al., 2019. Oxytocin alters patterns of brain activity and amygdalar connectivity by age during dynamic facial emotion identification. Neurobiol. Aging 78, 42–51.

Hu, K., Padmala, S., Pessoa, L., 2013. Interactions between reward and threat during visual processing. Neuropsychologia 51 (9), 1763–1772.

Ince, S., Steward, T., Harrison, B.J., Jamieson, A.J., Davey, C.G., Agathos, J.A., Moffat, B. A., Glarin, R.K., Felmingham, K.L., 2023. Subcortical contributions to salience network functioning during negative emotional processing. Neuroimage 270, 119964.

IsHak, W.W., Kahloon, M., Fakhry, H., 2011. Oxytocin role in enhancing well-being: a literature review. J. Affect. Disord. 130 (1–2), 1–9.

Jones, C., Barrera, I., Brothers, S., Ring, R., Wahlestedt, C., 2017. Oxytocin and social functioning. Dialogues Clin. Neurosci. https://doi.org/10.31887/dcns.2017.19.2/cjones.

Kirkpatrick, M.G., Lee, R., Wardle, M.C., Jacob, S., De Wit, H., 2014. Effects of MDMA and intranasal oxytocin on social and emotional processing. Neuropsychopharmacology 39 (7), 1654–1663.

Kirsch, P., 2015. Oxytocin in the socioemotional brain: implications for psychiatric disorders. Dialogues Clin. Neurosci. 17 (4), 463–476.

Koch, S.B.J., van Zuiden, M., Nawijn, L., Frijling, J.L., Veltman, D.J., Olff, M., 2019. Effects of intranasal oxytocin on distraction as emotion regulation strategy in patients with post-traumatic stress disorder. Eur. Neuropsychopharmacol 29 (2), 266–277.

Koch, S.B., van Zuiden, M., Nawijn, L., Frijling, J.L., Veltman, D.J., Olff, M., 2016. Intranasal oxytocin administration dampens amygdala reactivity towards emotional faces in male and female PTSD patients. Neuropsychopharmacology 41 (6), 1495–1504.

Kou, J., Zhang, Y., Zhou, F., Gao, Z., Yao, S., Zhao, W., Li, H., Lei, Y., Gao, S., Kendrick, K. M., 2022. Anxiolytic effects of chronic intranasal oxytocin on neural responses to threat are dose-frequency dependent. Psychother. Psychosom. 1–12.

Li, S.C., Rieckmann, A., 2014. Neuromodulation and aging: implications of aging neuronal gain control on cognition. Curr. Opin. Neurobiol. 29, 148–158.

Liu, P., Lin, T., Feifel, D., Ebner, N.C., 2022. Intranasal oxytocin modulates the salience network in aging. Neuroimage 253, 119045.
Luber, B., Lisanby, S.H., 2014. Enhancement of human cognitive performance using transcranial magnetic stimulation (TMS). Neuroimage 85, 961–970.
Luo, C., Li, Q., Xia, Y., Lei, X., Xue, K., Yao, Z., Lai, Y., Martí nez-Montes, E., Liao, W., Zhou, D., 2012. Resting state basal ganglia network in idiopathic generalized epilepsy. Hum. Brain Mapp. 33 (6), 1279–1294.
Maldjian, J.A., Laurienti, P.J., Kraft, R.A., Burdette, J.H., 2003. An automated method for neuroanatomic and cytoarchitectonic atlas-based interrogation of fMRI data sets. Neuroimage 19 (3), 1233–1239.
Martins, D., Paduraru, M., Paloyelis, Y., 2022. Heterogeneity in response to repeated intranasal oxytocin in schizophrenia and autism spectrum disorders: a meta-analysis of variance. Br. J. Pharmacol. 179 (8), 1525–1543.
Mary, A., Wens, V., Op de Beeck, M., Leproult, R., De Tiege, X., Peigneux, P., 2017. Age-related differences in practice-dependent resting-state functional connectivity related to motor sequence learning. Hum. Brain Mapp. 38 (2), 923–937.
Matsushita, H., Latt, H.M., Koga, Y., Nishiki, T., Matsui, H., 2019. Oxytocin and stress: neural mechanisms, stress-related disorders, and therapeutic approaches. Neuroscience 417, 1–10.
Menon, V., 2015. Salience network introduction and overview. Brain Mapping. https://doi.org/10.1016/B978-0-12-397025-1.00052-X.
Menon, V., Uddin, L.Q., 2010. Saliency, switching, attention and control: a network model of insula function. Brain Struct. Funct. 214, 655–667.
Meyer-Lindenberg, A., Domes, G., Kirsch, P., Heinrichs, M., 2011. Oxytocin and vasopressin in the human brain: social neuropeptides for translational medicine. Nat. Rev. Neurosci. 12 (9), 524–538.
Moerkerke, M., Daniels, N., Tibermont, L., Tang, T., Evenepoel, M., Van der Donck, S., et al., 2024. Chronic oxytocin administration stimulates the oxytocinergic system in children with autism. Nat. Commun. 15 (1), 58.
Naveau, M., Doucet, G., Delcroix, N., Petit, L., Zago, L., Crivello, F., et al., 2012. A novel group ICA approach based on multi-scale individual component clustering. Application to a large sample of fMRI data. Neuroinformatics 10, 269–285.
Paloyelis, Y., Doyle, O.M., Zelaya, F.O., Maltezos, S., Williams, S.C., Fotopoulou, A., Howard, M.A., 2016. A spatiotemporal profile of in vivo cerebral blood flow changes following intranasal oxytocin in humans. Biol. Psychiatr. 79 (8), 693–705.
Passow, S., Specht, K., Adamsen, T.C., Biermann, M., Brekke, N., Craven, A.R., Ersland, L., Grüner, R., Kleven-Madsen, N., Kvernenes, O., 2015. Default-mode network functional connectivity is closely related to metabolic activity. Hum. Brain Mapp. 36 (6), 2027–2038.
Peters, S., Slattery, D.A., Uschold-Schmidt, N., Reber, S.O., Neumann, I.D., 2014. Dose-dependent effects of chronic central infusion of oxytocin on anxiety, oxytocin receptor binding and stress-related parameters in mice. Psychoneuroendocrinology 42, 225–236.
Phung, L.C., Farrington, E.K., Connolly, M., Wilson, A.N., Carvalho, B., Homer, C.S., Vogel, J.P., 2021. Intravenous oxytocin dosing regimens for postpartum hemorrhage prevention following cesarean delivery: a systematic review and meta-analysis. Am. J. Obstet. Gynecol. 225 (3), 250 e1.
Power, J.D., Cohen, A.L., Nelson, S.M., Wig, G.S., Barnes, K.A., Church, J.A., et al., 2011. Functional network organization of the human brain. Neuron 72 (4), 665–678.
Quintana, D.S., Smerud, K.T., Andreassen, O.A., Djupesland, P.G., 2018. Evidence for intranasal oxytocin delivery to the brain: recent advances and future perspectives. Ther. Deliv. https://doi.org/10.4155/tde-2018-0002.
Raichle, M.E., 2015. The brain's default mode network. Annu. Rev. Neurosci. 38, 433–447.
Reed, S.C., Haney, M., Manubay, J., Campagna, B.R., Reed, B., Foltin, R.W., Evans, S.M., 2019. Sex differences in stress reactivity after intranasal oxytocin in recreational cannabis users. Pharmacol. Biochem. Behav. https://doi.org/10.1016/j.pbb.2018.11.008.
Riem, M.M., Bakermans-Kranenburg, M.J., Pieper, S., Tops, M., Boksem, M.A., Vermeiren, R.R., et al., 2011. Oxytocin modulates amygdala, insula, and inferior frontal gyrus responses to infant crying: a randomized controlled trial. Biol. Psychiatr. 70 (3), 291–297.
Rilling, J.K., DeMarco, A.C., Hackett, P.D., Chen, X., Gautam, P., Stair, S., Haroon, E., Thompson, R., Ditzen, B., Patel, R., Pagnoni, G., 2014. Sex differences in the neural and behavioral response to intranasal oxytocin and vasopressin during human social interaction. Psychoneuroendocrinology. https://doi.org/10.1016/j.psyneuen.2013.09.022.
Rissanen, J., 1983. A universal prior for integers and estimation by minimum description length. Ann. Stat. 11 (2), 416–431.
Röcke, C., Li, S.C., Smith, J., 2009. Intraindividualvariability in positive and negative affect over 45 days: do older adults fluctuate less than youngadults? Psychol. Aging 24, 863. https://doi.org/10.1037/A0016276.
Rocchetti, M., Radua, J., Paloyelis, Y., Xenaki, L.A., Frascarelli, M., Caverzasi, E., et al., 2014. Neurofunctional maps of the 'maternal brain'and the effects of oxytocin: a multimodal voxel-based meta-analysis. Psychiatr. Clin. Neurosci. 68 (10), 733–751.
Rolls, E.T., 2019. The cingulate cortex and limbic systems for emotion, action, and memory. Brain Struct. Funct. 224 (9), 3001–3018.
Rubbert, C., Mathys, C., Jockwitz, C., Hartmann, C.J., Eickhoff, S.B., Hoffstaedter, F., Caspers, S., Eickhoff, C.R., Sigl, B., Teichert, N.A., 2019. Machine-learning identifies Parkinson's disease patients based on resting-state between-network functional connectivity. Br. J. Radiol. 92 (1101), 20180886.
Rung, J.M., Horta, M., Tammi, E.M., Perez, E., Ojeda, M.C., Lin, T., et al., 2021. Safety and tolerability of chronic intranasal oxytocin in older men: results from a randomized controlled trial. Psychopharmacology 238 (9), 2405–2418.
Sannino, S., Chini, B., Grinevich, V., 2017. Lifespan oxytocin signaling: maturation, flexibility, and stability in newborn, adolescent, and aged brain. Developmental Neurobiology 77 (2), 158–168.
Schilbach, L., Eickhoff, S.B., Rotarska-Jagiela, A., Fink, G.R., Vogeley, K., 2008. Minds at rest? Social cognition as the default mode of cognizing and its putative relationship to the "default system" of the brain. Conscious. Cognit. 17 (2), 457–467.
Schmitz, T.W., Johnson, S.C., 2006. Self-appraisal decisions evoke dissociated dorsal-ventral aMPFC networks. Neuroimage. https://doi.org/10.1016/j.neuroimage.2005.10.030.
Shi, L., Sun, J., Xia, Y., Ren, Z., Chen, Q., Wei, D., et al., 2018. Large-scale brain network connectivity underlying creativity in resting-state and task fMRI: cooperation between default network and frontal-parietal network. Biol. Psychol. 135, 102–111.
Simmons, W.K., Avery, J.A., Barcalow, J.C., Bodurka, J., Drevets, W.C., Bellgowan, P., 2013. Keeping the body in mind: insula functional organization and functional connectivity integrate interoceptive, exteroceptive, and emotional awareness. Hum. Brain Mapp. 34 (11), 2944–2958.
Sippel, L.M., Allington, C.E., Pietrzak, R.H., Harpaz-Rotem, I., Mayes, L.C., Olff, M., 2017. Oxytocin and stress-related disorders: neurobiological mechanisms and treatment opportunities. Chronic stress 1, 2470547016687996.
Sripada, C.S., Phan, K.L., Labuschagne, I., Welsh, R., Nathan, P.J., Wood, A.G., 2013. Oxytocin enhances resting-state connectivity between amygdala and medial frontal cortex. Int. J. Neuropsychopharmacol. https://doi.org/10.1017/S1461145712000533.
Sun, J., Zhang, Q., Li, Y., Meng, J., Chen, Q., Yang, W., et al., 2020. Plasticity of the resting-state brain: static and dynamic functional connectivity change induced by divergent thinking training. Brain imaging and behavior 14, 1498–1506.
Szewczyk-Krolikowski, K., Menke, R.A.L., Rolinski, M., Duff, E., Salimi-Khorshidi, G., Filippini, N., Zamboni, G., Hu, M.T.M., Mackay, C.E., 2014. Functional connectivity in the basal ganglia network differentiates PD patients from controls. Neurology 83 (3), 208–214.
Uddin, L.Q., 2016. Salience Network of the Human Brain. Academic press.
Valdes-Hernandez, P.A., Polk, R., Horta, M., Frazier, I., Perez, E., Ojeda, M., Porges, E., Cruz-Almeida, Y., Feifel, D., Ebner, N.C., 2021. Chronic oxytocin administration in older men modulates functional connectivity during animacy perception. Aging Brain 1, 100023.
Varangis, E., Razlighi, Q., Habeck, C.G., Fisher, Z., Stern, Y., 2019. Between-network functional connectivity is modified by age and cognitive task domain. J. Cognit. Neurosci. 31 (4), 607–622.
Wager, T.D., Davidson, M.L., Hughes, B.L., Lindquist, M.A., Ochsner, K.N., 2008. Prefrontal-subcortical pathways mediating successful emotion regulation. Neuron 59 (6), 1037–1050.
Watanabe, T., Kuroda, M., Kuwabara, H., Aoki, Y., Iwashiro, N., Tatsunobu, N., Takao, H., Nippashi, Y., Kawakubo, Y., Kunimatsu, A., Kasai, K., Yamasue, H., 2015. Clinical and neural effects of six-week administration of oxytocin on core symptoms of autism. Brain. https://doi.org/10.1093/brain/awv249.
Watson, D., Clark, L.A., Tellegen, A., 1988. Development and validation of brief measures of positive and negative affect: the PANAS scales. J. Pers. Soc. Psychol. 54 (6), 1063.
Yamasue, H., 2016. Promising evidence and remaining issues regarding the clinical application of oxytocin in autism spectrum disorders. Psychiatr. Clin. Neurosci. 70 (2), 89–99.
Ye, Z., Donamayor, N., Muente, T.F., 2014. Brain network of semantic integration in sentence reading: insights from independent component analysis and graph theoretical analysis. Hum. Brain Mapp. 35 (2), 367–376.
Zanos, P., Wright, S.R., Georgiou, P., Yoo, J.H., Ledent, C., Hourani, S.M., Kitchen, I., Winsky-Sommerer, R., Bailey, A., 2014. Chronic methamphetamine treatment induces oxytocin receptor up-regulation in the amygdala and hypothalamus via an adenosine A2A receptor-independent mechanism. Pharmacol. Biochem. Behav. 119, 72–79.
Zhao, W., Yao, S., Li, Q., Geng, Y., Ma, X., Luo, L., Xu, L., Kendrick, K.M., 2016. Oxytocin blurs the self-other distinction during trait judgments and reduces medial prefrontal cortex responses. Hum. Brain Mapp. 37 (7), 2512–2527.
Zheng, S., Punia, D., Wu, H., Liu, Q., 2021. Graph theoretic analysis reveals intranasal oxytocin induced network changes over frontal regions. Neuroscience 459, 153–165.
Zhuang, Q., Zheng, X., Yao, S., Zhao, W., Becker, B., Xu, X., Kendrick, K.M., 2022. Oral administration of oxytocin, like intranasal administration, decreases top-down social attention. Int. J. Neuropsychopharmacol. 25 (11), 912–923.